

ORIGINAL ARTICLE OPEN ACCESS

Cost of Sensing in Optimal Control: Basic Formulations, Examples, and Applications

Dung Tran | Tri Ngo | Tuhin Das

Department of Mechanical and Aerospace Engineering, University of Central Florida, Orlando, Florida, USA |

Correspondence: Dung Tran (Dung.Tran@ucf.edu) | Tuhin Das (Tuhin.Das@ucf.edu)**Received:** Added at production | **Revised:** Added at production | **Accepted:** Added at production**Academic Editor:** ... | **Guest Editor:** ...**Keywords:** Sensing-Cost, Optimal Control, Two-Point Boundary Value Problem (TPBVP), Pontryagin's Minimum Principle, Shrinking Horizon

ABSTRACT

Incorporating a notion of cost of sensing, or sensing-cost, within the optimal control framework is beneficial in controlling systems where the duration of sensing, and/or the cost of sensors themselves, have a considerable impact on the overall cost. In this regard, this paper presents multiple methods for incorporating an integral sensing-cost into the optimal control framework for Linear Time-Invariant (LTI) systems. Sensing-cost is traded off against the conventional costs of control and stabilization. Optimal sensing intervals are derived by applying the Pontryagin's Minimum Principle. Other formulations of the sensing-cost problem, and extension to nonlinear systems, are possible. The theoretical developments of this paper are validated through numerical solutions and demonstrated through simulations. A reduced-form expression for the infinite-horizon multi-dimensional case with single switching point is derived, and a closed-form solution is obtained for the infinite-horizon first-order case. Additionally, a Shrinking Horizon method is demonstrated for practical implementation of the proposed theory and as a means to address uncertainties. A practical case study of a wastewater treatment plant is introduced to examine the applicability of sensing-cost considerations in a real-world setting.

1 | Introduction

In conventional optimal control problems, such as in LQR, the performance index typically weighs transient performance vs. control effort. An additional consideration can be the cost of sensing. Cost of sensing, or alternately sensing-cost, plays a pivotal role in shaping the overall design, implementation, and performance of control systems. It encompasses various aspects, including the price of sensors, the computational overhead associated with sensing and processing, energy consumption, and impacts on system complexity and reliability. This paper aims to explore the implications of incorporating sensing-cost within the optimal control framework, summarizing basic formulations, key methodologies, and findings.

Incorporation of sensing-cost within optimal control has not been reported in the literature. However, due to their ubiquitousness and practicality in control systems, numerous works have addressed various facets of sensing, such as sensor placement,

scheduling, sampling, etc. While such works are not directly relevant to this paper, we discuss selected ones from literature to put this work in context. For instance, [1] propose optimization techniques for sensor placement, employing greedy algorithms to achieve cost-effective configurations that maintain desired performance. In [2], the authors propose the concept of shared-sensing for reversible transducers that are continuously switched between actuator and sensor modes. The authors in [3] introduce a method to reduce the cost and power requirements of sensing while streamlining data storage and processing in vibration-based monitoring and diagnostics using compressive sensing. In [4], the authors address collaborative sensing with the goal of determining a sensor schedule that minimizes the error covariance. In [5], the authors address a sensor scheduling problem that involves estimating the state of an uncertain process using measurements obtained by sequentially switching among a set of noisy sensors. A work which has some conceptual similarity with that presented in this paper is [6]. Here, the authors introduce event-triggered

and self-triggered control systems. Event-triggered control is reactive, initiating sensor sampling and control actions when the system state deviates beyond a predefined threshold. In contrast, self-triggered control takes a proactive approach, predicting the next sampling or actuation instance in advance. The paper demonstrates how these control techniques can be implemented, with examples from applications in the process industry. In this work, the states are sensed regularly to detect triggering, while action (i.e., control computation and new actuation) may only take place when triggered.

In many real-world systems, the challenge lies not in sensor availability but in the cost of continuous sensing—whether in energy consumption, bandwidth usage, signal processing/computational cost or operational constraints. Battery-powered UAVs, underwater autonomous vehicles, wireless sensor networks, and planetary rovers all operate under strict power budgets, where high-frequency sensing (e.g., LiDAR, sonar) can significantly shorten mission duration. Similarly, in networked control systems—often with battery-operated sensors deployed in remote locations—communication costs further constrain sensing schedules, forcing control designers to explicitly consider when sensors should be activated. For example, in [7], the authors quantify the trade-off between the cost of activating expensive sensors and the resulting improvement in observation accuracy. In such cases, the control agents' task extends beyond stabilizing system states to also accounting for sensing-costs, with the aim of minimizing the overall operational costs. Optimizing sensing intervals in these contexts is therefore critical to extending mission longevity and maintaining system performance.

However, there is no rigorous study that directly incorporates sensing-cost into the optimal control problem, as proposed in this paper. This approach jointly accounts for sensing-cost, control effort, and state stabilization, ensuring a trade-off between system performance and resource utilization. Here, we present the fundamental formulations of sensing-cost, along with simple examples to illustrate the theoretical development. The contributions of this paper are:

1. We propose a unified optimization framework that explicitly includes sensing-cost alongside control effort and state stabilization in the cost functional. This framework enables the systematic evaluation of the trade-offs between these competing objectives, addressing the limitations of traditional control design approaches that treat cost of sensing as a secondary concern or ignore it altogether.
2. A binary switching variable is used to toggle state sensing on and off. Switching is optimized to minimize the cost functional, determining the optimal sequence of sensing actions based on system dynamics and desired performance criteria. We employ the Pontryagin's Minimum Principle to derive the necessary conditions for optimality.
3. The proposed framework is validated through numerical simulations, demonstrating its effectiveness in balancing sensing-cost and control performance. A Shrinking Horizon approach is demonstrated, providing a practical alternative to implementing the resulting Two-Point Boundary Value Problems (TPBVPs).

The remainder of the paper is organized as follows. Section 2 defines the problem, introducing the system model, cost functional, and constraints. In Section 3, the theoretical development of the proposed framework is detailed, including the derivation

of optimality conditions using Pontryagin's Minimum Principle. Section 4 examines a specific case of the sensing cost framework for which an analytical expression can be derived for the infinite-horizon optimal problem. This section also presents a closed-form solution for the first-order infinite-horizon case. Numerical examples showcasing the effectiveness of the approach across various scenarios are presented in Section 5. To address practical implementation challenges, Section 6 presents an example of incorporating sensing cost into a wastewater treatment plant and Section 7 introduces a Shrinking Horizon method for dynamic optimization under uncertainties. Finally, Section 8 provides concluding remarks and outlines directions for future research.

2 | Problem Statement

Consider a Linear Time Invariant (LTI) system,

$$\dot{X} = AX + Bu, \quad X \in \mathbb{R}^n, \quad u \in \mathbb{R}^m \quad (1)$$

Consider the design of a controller for this system under the condition that sensing of the states X can be switched on or off. We define a scalar switching variable z as follows,

$$z = \begin{cases} 1 & \text{when sensing is on} \\ 0 & \text{when sensing is off} \end{cases} \quad (2)$$

When $z = 1$, we consider two types of input formulations,

$$z = 1 \Rightarrow \begin{cases} \text{Case 1: Predefined state feedback } u = -KX \\ \text{Case 2: Optimal formulation } u^* \end{cases} \quad (3)$$

Similarly, when $z = 0$ we consider the following two types of input formulations,

$$z = 0 \Rightarrow \begin{cases} \text{Case 1: } \dot{u} = [0] \\ \text{Case 2: } u = [0] \end{cases} \quad (4)$$

We impose that z must be switched to minimize the cost functional,

$$J = \int_{t_0}^{t_f} L(X, u, z) dt \quad (5)$$

where t_f is a fixed final time. Based on the above problem statement, in the next section we formulate three specific optimal control problems, with examples provided in subsequent sections. Each of the three problems incorporates the cost of sensing and provides a switching law for z .

3 | Theoretical Development

3.1 | Input u Held Constant when $z = 0$ and $u = -KX$ when $z = 1$

In this scenario, we formulate the u as follows:

$$u = -KX \text{ when } z = 1 \text{ and } \dot{u} = 0 \text{ when } z = 0 \quad (6)$$

where K is a predefined gain matrix. From Eq.(6), the derivative of u can be written as,

$$\dot{u} = -zK(AX + Bu) \quad (7)$$

We have the augmented state vector $\bar{X} = [X \ u]^T$ and the following augmented state equation,

$$\dot{\bar{X}} = f(\bar{X}, z) = \begin{bmatrix} A & B \\ -zKA & -zKB \end{bmatrix} \bar{X} \quad (8)$$

The objective is to minimize the cost functional,

$$J = \int_{t_0}^{t_f} (X^T Q X + sz) dt \quad (9)$$

where Q is symmetric positive semi-definite, and $s > 0$. We clarify that since a predefined state feedback control is used, Case 1 in Eq.(3), hence J does not include a $u^T R u$, $R > 0$ term. Equation (9) can be expressed as,

$$J = \int_{t_0}^{t_f} (\bar{X}^T \bar{Q} \bar{X} + sz) dt, \quad \bar{Q} = \begin{bmatrix} Q & 0 \\ 0 & 0 \end{bmatrix} \quad (10)$$

We note in Eq.(9) that the term $\int_{t_0}^{t_f} sz dt$ imposes a sensing-cost. It is distinct from control cost $\int_{t_0}^{t_f} u^T R u dt$ in that s adds to the cost whenever $z = 1$, irrespective of the control input u . The Hamiltonian is:

$$H = L + \lambda^T f = \bar{X}^T \bar{Q} \bar{X} + sz + \lambda^T \begin{bmatrix} A & B \\ -zKA & -zKB \end{bmatrix} \bar{X} \quad (11)$$

In Eq.(11), $\lambda = [\lambda_x \ \lambda_u]^T$ is an $(n+m)$ -element vector of Lagrange multipliers. To determine a condition for switching z , we apply the Pontryagin's minimum principle ([8, 9, 10, 11]), which is a necessary condition for optimality. In the context of this problem, it states that the Hamiltonian must be minimized over the admissible region of z for optimal values of the state and co-state. Since z is constrained to assume discrete integer values, the Pontryagin's minimum principle cannot be directly applied. To address this issue, we allow z to vary continuously in the admissible range $[0, 1]$. Thereby, we embed our switched system within a larger family of systems, as done in [12]. For the admissible range of z , i.e., $z \in [0, 1]$, a necessary condition for optimality is found by minimizing the Hamiltonian H , Eq.(11). Thus,

$$H(\bar{X}^*, \lambda^*, z^*) \leq H(\bar{X}^*, \lambda^*, z) \quad \forall t \in [t_0, t_f] \quad (12)$$

for all admissible z . We note from Eq.(11) that,

$$H = \bar{X}^T \bar{Q} \bar{X} + sz + \lambda_x^T [A \ B] \bar{X} - z \lambda_u^T K [A \ B] \bar{X} \quad (13)$$

is linear in z for any \bar{X}^* and λ^* . Therefore, z^* lies at the discrete points $\{0, 1\}$ for all $t \in [t_0, t_f]$, and the formulation of u in Eq.(6) is valid at all instants. The solution $z^* = 0$ minimizes H if,

$$\begin{aligned} & H(\bar{X}^*, \lambda^*, z) \Big|_{z=0} < H(\bar{X}^*, \lambda^*, z) \Big|_{z=1} \\ \Leftrightarrow & \bar{X}^{*T} \bar{Q} \bar{X}^* + \lambda_x^{*T} [A \ B] \bar{X}^* < \dots \\ & \bar{X}^{*T} \bar{Q} \bar{X}^* + s + \lambda_x^{*T} [A \ B] \bar{X}^* - \lambda_u^{*T} K [A \ B] \bar{X}^* \\ \Leftrightarrow & \lambda_u^{*T} K [A \ B] \bar{X}^* < s \Leftrightarrow \lambda_u^{*T} K (A \bar{X}^* + B u^*) < s \end{aligned} \quad (14)$$

Similarly, $z^* = 1$ minimizes H if $\lambda_u^{*T} K (A \bar{X}^* + B u^*) \geq s$. Thus, in the sense of minimizing H for all admissible z , the condition

for optimal switching between sensing ($z = 1$) and no-sensing ($z = 0$) is,

$$z^* = \begin{cases} 0 & \text{if } \lambda_u^T K (A X + B u) < s \\ 1 & \text{if } \lambda_u^T K (A X + B u) \geq s \end{cases} \quad (15)$$

We note that Eq.(15) is a necessary condition for optimality. The co-states equation and boundary conditions are:

$$\dot{\lambda} = -\frac{\partial H}{\partial \bar{X}} = -2\bar{Q}\bar{X} - \begin{bmatrix} A^T & -zA^T K^T \\ B^T & -zB^T K^T \end{bmatrix} \lambda \quad (16)$$

$$\bar{X}(t_0) = [X_0^T \ -X_0^T K^T]^T, \quad \lambda(t_f) = \frac{\partial \phi}{\partial \bar{X}}(t_f) = [0] \quad (17)$$

where $\phi(X(t_f), t_f)$ is the final weighting function, which is set to zero in this study. Equations (8), (15), (16) and (17) form a Two-Point Boundary Value Problem (TPBVP) that can be solved by numerical methods such as the "Shooting Method" or the "Relaxation Method" ([13, 14]).

Observations

We note the possibility of *singular intervals*, [8, 10], if the criterion,

$$\lambda_u^T K (A X + B u) = s \quad (18)$$

is satisfied over a finite interval $t \in [t_1, t_2]$. Another necessary condition for optimality is that if the Hamiltonian is not an explicit function of time, then it is constant along the optimal trajectory for a fixed final-time problem, [8, 10]. This necessary condition implies,

$$\begin{aligned} \dot{H} &= \left(\frac{\partial H}{\partial \bar{X}} \right)^T \dot{\bar{X}} + \left(\frac{\partial H}{\partial \lambda} \right)^T \dot{\lambda} + \frac{\partial H}{\partial z} \dot{z} \\ &= -\dot{\lambda}^T \dot{\bar{X}} + \dot{\bar{X}}^T \dot{\lambda} + \frac{\partial H}{\partial z} \dot{z} \\ &= [s - \lambda_u^T K (A X + B u)] \dot{z} = 0 \end{aligned} \quad (19)$$

From Eqs.(18) and (19), we conclude that outside of singular intervals, $\dot{z} = 0$ along optimal trajectories. This confirms that for the proposed problem, where $z \in [0, 1]$, optimality occurs necessarily at the discrete points, $z \in \{0, 1\}$ outside of singular intervals. From Eq.(18), a necessary condition for the existence of a singular interval is,

$$\frac{d}{dt} (s - \lambda_u^T K (A X + B u)) = 0 \Rightarrow [\lambda_x^T B K - \lambda_u^T K A] \dot{X} = 0 \quad (20)$$

over a finite interval $t \in [t_1, t_2]$. While the above condition does not provide much insight into the singular input z , for a scalar system further deductions can be made. For a scalar system, if we represent A , B , K , and X by their scalar equivalents a , b , k , and x , then Eq.(20) reduces to

$$(\lambda_x b - \lambda_u a) \dot{x} = 0$$

which implies a necessary condition for the existence of singular arcs is either $(\lambda_x b - \lambda_u a) = 0$, or $\dot{x} = 0$, or both over a finite interval $t \in [t_1, t_2]$. The former condition can be further differentiated with respect to time to yield the following necessary condition:

$$\frac{d}{dt} (\lambda_x b - \lambda_u a) = 0 \Rightarrow -2bqx = 0 \quad (21)$$

where q is the scalar equivalent of Q defined in Eq.(9). Assuming the parameters a, b, q, k to be non-zero, Eq.(21) implies $x = 0$ in $t \in [t_1, t_2]$, which implies $\dot{x} = 0, \ddot{x} = 0$, and so on for higher derivatives in $t \in [t_1, t_2]$. Equation (21) still does not produce any condition on z for a singular solution. However, upon differentiation of \dot{x} , we have,

$$\ddot{x} = (a - bkz)\dot{x} \quad (22)$$

which implies $z^* = a/(bk)$ is a necessary condition for optimality in a singular interval $t \in [t_1, t_2]$. Thus, for the scalar version, limiting $z \in \{0, 1\}$ (i.e., sensing vs. no-sensing conditions) in a singular interval may yield sub-optimal solutions.

A second observation is regarding the inclusion of input/control cost $u^T R u$, $R > 0$, in Eq.(9). If done, then in Eq.(10) $\bar{Q} = [Q \ 0; 0 \ R]$, and the derivation from Eq.(14) to Eq.(17) would remain unchanged. However, as mentioned after Eq.(9), since a predefined state feedback control is used, we do not include this term in J . Simulations reveal that if incorporated, it complicates the convergence of TPBVP solutions, and hence requires further investigations.

3.2 | Input $u = [0]$ when $z = 0$ and $u = -KX$ when $z = 1$

The method presented in section 3.1 has a disadvantage in that it increases the order of the state equation by m . Therefore, the complexity of calculations also increases. This is avoided by imposing the control input to be zero when the states are not sensed, i.e., $u = [0]$ when $z = 0$, as in Case 2 of Eq.(4). The objective is to minimize the cost functional of Eq.(9), since u is still a predetermined input. The state equation takes the form,

$$\dot{X} = f(X, z) = (A - zBK)X \quad (23)$$

and the Hamiltonian is,

$$H = L + \lambda^T f = X^T Q X + sz + \lambda^T (A - zBK)X \quad (24)$$

As in Section 3.1, for admissible values of z , i.e. $z \in \{0, 1\}$, the optimal z is found by first embedding our switched system within a larger family of systems where $z \in [0, 1]$. Thereafter, we minimize the Hamiltonian H , Eq.(24), according to the Pontryagin's minimum principle. Proceeding as in Section 3.1, the condition for optimal switching between sensing ($z = 1$) and no-sensing ($z = 0$) is,

$$z^* = \begin{cases} 0 & \text{if } \lambda^T B K X < s \\ 1 & \text{if } \lambda^T B K X \geq s \end{cases} \quad (25)$$

The co-states equation and boundary conditions are:

$$\dot{\lambda} = -\frac{\partial H}{\partial X} = -2QX - (A - zBK)^T \lambda \quad (26)$$

$$X(t_0) = X_0, \quad \lambda(t_f) = \frac{\partial \phi}{\partial X}(t_f) = [0] \quad (27)$$

Equations (23), (25), (26) and (27) form a TPBVP that can be solved numerically.

As in Section 3.1, a singular interval occurs if $\lambda^T B K X = s$ over a finite interval $t \in [t_1, t_2]$. A necessary condition for the existence of a singular interval is therefore,

$$\frac{d}{dt} (\lambda^T B K X) = 2X^T Q B K X + \lambda^T (A B K - B K A) X = 0 \quad (28)$$

Again, Eq.(28) does not provide insight into the singular input z . Similar to Section 3.1, further deductions can however be made for the scalar case. Representing A, B, K, Q and X by their scalar equivalents, a, b, k, q , and x , Eq.(28) reduces to $2qb k x^2 = 0$. Therefore, the necessary conditions for the existence of a singular interval are, $x = 0, \dot{x} = 0, \ddot{x} = 0$, and so on, in that interval. We note from Eq.(23) that $z^* = a/(bk)$ ensures $\dot{x} = 0$, and is thus a necessary condition for optimality in singular intervals. Thus, for the scalar version, limiting $z \in \{0, 1\}$, as proposed in Eq.(25), albeit practical, may yield sub-optimal solutions in a singular interval. Finally, an input/control cost $u^T R u$, $R > 0$, can be incorporated in Eq.(9) by modifying J as follows:

$$J = \int_{t_0}^{t_f} (X^T Q X + u^T R u + sz) dt = \int_{t_0}^{t_f} [X^T (Q + zQ_2) X + sz] dt \quad (29)$$

where, $Q_2 = K^T R K$. However, as mentioned just before Eq.(23), we have not considered the control cost since u is a predefined input. As in Section 3.1, here also simulations reveal that if included, this term complicates the convergence of TPBVP solutions. This will be an area of future investigations.

3.3 | Input $u = [0]$ when $z = 0$ and Optimal Input $u = u^*$ when $z = 1$

Here, we continue to impose u in Eq.(1) to be set at $u = [0]$ when the sensors are disabled (i.e., $z = 0$). This corresponds to Case 2 of Eq.(4), as in Section 3.2. However, unlike Section 3.2, the objective here is to use an optimal control u^* when $z = 1$. This refers to Case 2 of Eq.(3). The state equation takes the form,

$$\dot{X} = AX + zBu \quad (30)$$

The goal is to minimize the cost functional of Eq.(5), with the specific form,

$$J = \int_{t_0}^{t_f} (X^T Q X + u^T R u + sz) dt \quad (31)$$

From Eqs.(30) and (31), the Hamiltonian is,

$$H = L + \lambda^T f = X^T Q X + u^T R u + sz + \lambda^T (AX + zBu) \quad (32)$$

As in Sections 3.1 and 3.2, for admissible values of z , i.e. $z \in \{0, 1\}$, the optimal z is found by first embedding our switched system within a larger family of systems where $z \in [0, 1]$. Thereafter, we minimize H , Eq.(32), according to the Pontryagin's minimum principle. The Hamiltonian is quadratic in the unconstrained input u . Since $R \in \mathbb{R}^{m \times m}$ is symmetric positive definite, therefore for a specific value of z , H has a minimum for all $u \in \mathbb{R}^m$ when,

$$\frac{\partial H}{\partial u} = 2Ru + zB^T \lambda = [0] \Rightarrow u_{min} = -\frac{1}{2} z R^{-1} B^T \lambda \quad (33)$$

Now, substituting the above expression of $u = u_{min}$ in Eq.(32), we have,

$$H|_{u_{min}} = X^T Q X + \lambda^T A X + sz - \frac{1}{4} z^2 \lambda^T B R^{-1} B^T \lambda \quad (34)$$

Note that $H|_{u_{min}}$ is a quadratic expression in z . Furthermore, $\frac{1}{4} \lambda^T B R^{-1} B^T \lambda > 0$ for all $\lambda \neq [0]$, since it has a quadratic form and

$R^{-1} > 0$ as R is positive definite and symmetric. Hence, $H|_{u_{min}}$ has a maximum at,

$$\frac{\partial H|_{u_{min}}}{\partial z} = 0 \Rightarrow z_{max} = \frac{2s}{\lambda^T B R^{-1} B^T \lambda} > 0$$

and is monotonically decreasing on either side of z_{max} . Therefore, within the admissible range $z \in [0, 1]$, H is minimized at one of the discrete values $z \in \{0, 1\}$. Thus, the optimal input, from Eq.(33), is,

$$u^* = u_{min} = -\frac{1}{2} z R^{-1} B^T \lambda \quad (35)$$

For choosing $z = z^*$, note that the necessary condition for optimality from the Pontryagin's minimum principle is,

$$H(X^*, \lambda^*, u^*, z^*) \leq H(X^*, \lambda^*, u^*, z) \quad \forall t \in [t_0, t_f]$$

Hence, we choose $z^* = 0$ when,

$$\begin{aligned} H|_{u_{min}, z=0} &< H|_{u_{min}, z=1} \\ \Leftrightarrow 0 < s - \frac{1}{4} \lambda^{*T} B R^{-1} B^T \lambda^* &\Leftrightarrow s > \frac{1}{4} \lambda^{*T} B R^{-1} B^T \lambda^* \end{aligned} \quad (36)$$

Thus, the condition for optimal switching between sensing ($z = 1$) and no-sensing ($z = 0$) is,

$$z^* = \begin{cases} 0 & \text{if } 0.25 \lambda^T B R^{-1} B^T \lambda < s \\ 1 & \text{if } 0.25 \lambda^T B R^{-1} B^T \lambda \geq s \end{cases} \quad (37)$$

Note that unlike in Sections 3.1 and 3.2, this scenario does not permit singular intervals. The co-states equation and boundary condition are:

$$\dot{\lambda} = -\frac{\partial H}{\partial X} = -2QX - A^T \lambda \quad (38)$$

$$X(t_0) = X_0, \quad \lambda(t_f) = \frac{\partial \phi}{\partial X}(t_f) = [0] \quad (39)$$

Equations (30), (35), (37), (38) and (39) form a TPBVP that can be solved numerically. In Section 5, we provide examples of the problems discussed in this section. We present numerical solutions as well as a practical "shrinking horizon implementation." In the next section, we analyze the sensing-cost problem for a first-order system.

4 | Infinite Time Case with Single Switching Instant

Scenarios where the sensing-cost problem admits only one switching instant under an infinite time horizon are considered in this section. Specifically, these scenarios are considered within the context of the problem formulation of Section 3.2, and analytical results are derived. Here, the optimal switching condition in given in Eq.(25). Define the switching function $\alpha(t) = \lambda^T(t) B K X(t)$, noting that $\alpha(t)$ is scalar. The time derivative of $\alpha(t)$ is:

$$\alpha = \lambda^T B K X \Rightarrow \dot{\alpha} = \left[\frac{\partial \alpha}{\partial \lambda} \right]^T \dot{\lambda} + \left[\frac{\partial \alpha}{\partial X} \right]^T \dot{X} = (B K X)^T \dot{\lambda} + (\lambda^T B K) \dot{X} \quad (40)$$

Substitute equations (23) and (26) into (40), we have:

$$\begin{aligned} \dot{\alpha} &= X^T K^T B^T \left[-2QX - (A - zBK)^T \lambda \right] + \lambda^T B K (A - zBK) X \\ &= -2X^T K^T B^T Q X - X^T K^T B^T A^T \lambda + z X^T (K^T B^T)^2 \lambda \\ &\quad + \lambda^T B K A X - z \lambda^T (BK)^2 X \\ &= -2X^T (QBK) X + \lambda^T (BKA - ABK) X \end{aligned} \quad (41)$$

From the equation above, we observe that if QBK is positive (or negative) definite (or semidefinite) and if A and BK commute, the optimal solution will have at most one switching point. In this regard, we state and prove the following Lemma,

Lemma 1. For the LTI system of Eq.(1) with a single input, i.e., $u \in \mathbb{R}^1$, for any $K \in \mathbb{R}^{1 \times n}$, a necessary condition for the matrices A and BK to commute is that the controllability matrix $C = [B \ AB \ \dots \ A^{n-1}B]$ has a rank of 1.

Proof: Note that,

$$BKB = B(KB) = \rho B, \quad \rho = KB \quad (42)$$

Thus, $\rho = KB$ is an eigenvalue of BK and B is the corresponding eigenvector. Since C is rank 1, therefore,

$$AB = \bar{\rho} B \quad (43)$$

Thus, $\bar{\rho}$ is an eigenvalue of A and B is the corresponding eigenvector. Hence, the matrices A and BK have corresponding eigenvalues of $\bar{\rho}$ and ρ with the common eigenvector B . Since two commuting matrices must have the same set of eigenvectors, [15], the above mentioned necessary condition is satisfied by the eigenvector B . \square

Let us assume that the following three conditions are valid,

1. A and $(A - BK)$ are Hurwitz
2. A and BK commute
3. QBK is positive semidefinite

Then, from Eq.(41), it is guaranteed that the optimal solution has at most one switching point. We denote the switching instant as t_{sw} . From Eq.(23), for $t \leq t_{sw}$, the system equation is $\dot{X} = (A - BK)X$ and the solution is, $X(t) = e^{(A-BK)t} X_0 \forall t \in [0, t_{sw}]$. The system switches to $\dot{X} = AX$ at $t = t_{sw}$, the solution in this interval is:

$$X(t) = e^{A(t-t_{sw})} X(t_{sw}) = e^{A(t-t_{sw})} e^{(A-BK)t_{sw}} X_0 \quad (44)$$

We have $e^{A(t-t_{sw})} = e^{At} e^{-At_{sw}}$, and because $A(A - BK) = A^2 - ABK = A^2 - BKA = (A - BK)A$ due to condition (2), we have from Eq.(44),

$$X(t) = e^{At} e^{-At_{sw}} e^{(A-BK)t_{sw}} X_0 = e^{At} e^{-BKt_{sw}} X_0 \quad (45)$$

Equation (41) now becomes,

$$\dot{\alpha} = -2X^T(t) (QBK) X(t) \quad (46)$$

Integrating $\dot{\alpha}$ from t_{sw} to ∞ , we have,

$$\int_{t_{sw}}^{\infty} -2X^T(t) (QBK) X(t) dt = \alpha(\infty) - \alpha(t_{sw}) \quad (47)$$

From Eqs.(25) and (40), we have $\alpha(t_{sw}) = s$. Furthermore, from Eq.(27) and because A is Hurwitz, we have,

$$\begin{cases} \lim_{t \rightarrow \infty} \lambda(t) = \mathbf{0}_{n \times 1} \\ \lim_{t \rightarrow \infty} X(t) = \mathbf{0}_{n \times 1} \end{cases} \Rightarrow \lim_{t \rightarrow \infty} \alpha(t) = 0$$

Thus, substituting (45) into (47), we have,

$$-2X_0^T e^{-K^T B^T t_{sw}} \left(\int_{t_{sw}}^{\infty} e^{A^T t} (QBK) e^{At} dt \right) e^{-BK t_{sw}} X_0 = -s \quad (48)$$

From the Lyapunov equation, because A is Hurwitz and $QBK \geq 0$, there exists a matrix $P \geq 0$ such that $A^T P + PA = -QBK$ [16]. Note that,

$$\begin{aligned} \frac{d}{dt} (e^{A^T t} P e^{At}) &= \frac{d}{dt} (e^{A^T t}) P e^{At} + e^{A^T t} P \frac{d}{dt} (e^{At}) \\ &= e^{A^T t} A^T P e^{At} + e^{A^T t} P A e^{At} \\ &= -e^{A^T t} (QBK) e^{At} \end{aligned} \quad (49)$$

Therefore, Eq.(48) reduces to,

$$\begin{aligned} &-2X_0^T e^{-K^T B^T t_{sw}} \int_{t_{sw}}^{\infty} d(-e^{A^T t} P e^{At}) e^{-BK t_{sw}} X_0 = -s \\ \Rightarrow &-2X_0^T e^{-K^T B^T t_{sw}} \left[\mathbf{0}_{n \times n} + e^{A^T t_{sw}} P e^{A t_{sw}} \right] e^{-BK t_{sw}} X_0 = -s \quad (50) \\ \Rightarrow &-2X_0^T e^{-K^T B^T t_{sw}} e^{A^T t_{sw}} P e^{A t_{sw}} e^{-BK t_{sw}} X_0 = -s \\ \Rightarrow &2X_0^T e^{(A-BK)^T t_{sw}} P e^{(A-BK) t_{sw}} X_0 = s \end{aligned}$$

For a multi-dimensional system, Eq.(50) is a transcendental equation which does not have a closed-form solution. However, since this equation has at most one solution, numerical methods can be used to find its root. We make the following remark:

Remark 1. Equation (50) is equivalently, $2X^T(t_{sw})PX(t_{sw}) = s$.

The above observation can be made from Eq.(45). Next, we propose a condition on s that guarantees the existence of a switching time t_{sw} . However, we first state and prove the following Lemma:

Lemma 2. *Let I be a real interval and let $f : I \mapsto \mathbb{R}$ be a continuous injective function. Then f is strictly monotonic.*

Proof: Suppose that f is not strictly monotonic. Then there exist $a, b, c \in I$ with $a < b < c$ such that either:

$$f(a) \leq f(b) \text{ and } f(b) \geq f(c)$$

or

$$f(a) \geq f(b) \text{ and } f(b) \leq f(c).$$

Without loss of generality, assume that $f(a) \leq f(b)$ and $f(b) \geq f(c)$. Since f is injective, the case $f(a) = f(b)$ implies $a = b$, which contradicts $a < b < c$. Hence, we must have $f(a) < f(b)$ and $f(b) > f(c)$. Let,

$$d = \frac{f(b) + \max\{f(a), f(c)\}}{2}$$

By the Intermediate Value Theorem, there exist $x_1 \in (a, b)$ and $x_2 \in (b, c)$ such that $f(x_1) = d$ and $f(x_2) = d$. Since $x_1 < b < x_2$ and $f(x_1) = f(x_2)$, this contradicts the injectivity of f . Therefore, f must be strictly monotonic. \square

Now, we state and prove the following Proposition:

Proposition 1. *Equation (50) admits a unique positive root if and only if $0 < s < 2X_0^T P X_0$.*

Proof: Let $f(t) = 2X_0^T e^{(A-BK)^T t} P e^{(A-BK)t} X_0$. The function $f(t)$ is continuous in t . Furthermore, under the assumption that QBK is positive semidefinite, the system admits at most one switching time. Hence, $f(t)$ is injective on $(0, +\infty)$. By Lemma 2, $f(t)$ is strictly monotonic on this interval. Since P is positive semidefinite and $(A - BK)$ is Hurwitz, we have:

$$\lim_{t \rightarrow 0^+} f(t) = 2X_0^T P X_0 \geq 0, \quad \lim_{t \rightarrow \infty} f(t) = 0.$$

Therefore, if $2X_0^T P X_0 > 0$, the function $f(t)$ is *bijective* from $(0, +\infty)$ to $(0, 2X_0^T P X_0)$. Hence, the equation $f(t) = s$ admits a unique solution if and only if $0 < s < 2X_0^T P X_0$. \square

We observe that, if A and $(A - BK)$ are Hurwitz, A and BK commute and if QBK is negative semidefinite, then the only optimal control is $z^*(t) = 0 \forall t$. This is because, for a negative semidefinite QBK , following the derivation of Eq.(50) and from Remark 1, we have, $2X^T(t_{sw})PX(t_{sw}) = -s$, which does not have a solution for $s > 0$. Thus, z^* does not undergo any switching. In this case, $z^*(t) = 0 \forall t$ is the only possibility for obtaining a finite cost. We end this section by making the following remark,

Remark 2. If $X_0^T P X_0 = 0$, then the optimal solution satisfies $z^*(t) = 0 \forall t$.

4.1 | Closed-Form Solution for First-order System

Extending the discussion so far in Section 4, we next explore some interesting characteristics of the optimal problem of Section 3.2 when posed for a first-order system. Consider the first order system,

$$\dot{x} = ax + bu \quad (51)$$

We assume that the parameters a and b , and the initial condition $x(0) = x_0 > 0$ are known. The control signal is, $u = -kzx$, where k is a constant positive feedback gain and z is the sensing state. From the characteristic of first-order systems, we observe that $x(t) \neq 0 \forall t$. The dynamical equation becomes,

$$\dot{x} = ax - bkzx = (a - bkz)x \quad (52)$$

The above structure conforms to the system of Section 3.2. The objective is to minimize the cost functional,

$$J = \int_0^{t_f} [(q_1 + q_2 z)x^2 + sz] dt \quad (53)$$

where $q_1 \geq 0$, $q_2 \geq 0$, and $s > 0$ are constant. In the equation above, q_1 is the coefficient associated with the state cost, while q_2 becomes active only when the state is sensed, i.e., when $z = 1$. The term $q_2 z x^2$ represents an input cost of the form given in Eq.(29). The Hamiltonian H is (λ is the Lagrange multiplier),

$$\begin{aligned} H &= (q_1 + q_2 z)x^2 + sz + \lambda(ax - bkzx) \\ &= q_1 x^2 + a\lambda x + z(q_2 x^2 + s - bk\lambda x) \end{aligned} \quad (54)$$

The Pontryagin's minimum principle is applied to minimize H with respect to z , by expanding the admissible range of z to the

interval $[0, 1]$, as done in Section 3. This yields,

$$\begin{aligned} H(x^*, \lambda^*, z^*) &\leq H(x^*, \lambda^*, z) \\ \Leftrightarrow z^*(q_2x^2 + s - bk\lambda x) &\leq z(q_2x^2 + s - bk\lambda x) \\ \Leftrightarrow z^* &= \begin{cases} 0 & \text{if } (q_2x^2 + s - bk\lambda x) > 0 \\ 1 & \text{if } (q_2x^2 + s - bk\lambda x) < 0 \\ \text{indeterminate} & \text{if } (q_2x^2 + s - bk\lambda x) = 0 \end{cases} \end{aligned} \quad (55)$$

Denoting $\alpha(t) = q_2x^2(t) + s - bk\lambda(t)x(t)$ to be the *switching function*, we observe that $z^*(t) = 0$ when $\alpha(t) > 0$ and $z^*(t) = 1$ when $\alpha(t) < 0$. The time derivative $\dot{\alpha}(t)$ is,

$$\dot{\alpha}(t) = (2q_2x - bk\lambda)\dot{x} - bkx\dot{\lambda} \quad (56)$$

The co-state equation is,

$$\begin{aligned} \dot{\lambda} &= -\frac{\partial H}{\partial x} = -2(q_1 + q_2z)x - \lambda(a - bkz) \\ &= -2(q_1 + q_2z)x - \lambda(a - bkz) \end{aligned} \quad (57)$$

Substituting Eqs.(52) and (57) into Eq.(56), we have,

$$\begin{aligned} \dot{\alpha} &= (2q_2x - bk\lambda)(a - bkz)x \\ &\quad - bkx[-2(q_1 + q_2z)x - \lambda(a - bkz)] \\ &= 2q_2(a - bkz)x^2 - bk\lambda x(a - bkz) + 2(q_1 + q_2z)bkx^2 \\ &\quad + bkx\lambda(a - bkz) \\ &= 2x^2[q_2(a - bkz) + (q_1 + q_2z)bk] = 2(q_1bk + q_2a)x^2 \end{aligned} \quad (58)$$

Note that since the system considered here is scalar, the commutativity requirement of Eq.(41) is not applicable in this case. In Eq.(58), since a, b, q_1, q_2 , and k are constants, it follows that the sign of $\dot{\alpha}(t)$ remains unchanged over time. Therefore, we can conclude that the optimal solution will have at most one switching point. Depending on the value of (a, b, k, q_1, q_2) , there are three possible cases listed in Table 1. Note that the switching time t_{sw} depends on a, b, k, q_1, q_2 , and t_f .

TABLE 1 | Optimal sensing sequences - first-order system

Case	$q_1bk + q_2a$	Possible optimal sequences
1	+	$z = 0 \forall t$ or $z = 1 \forall t$ or $z(t) = \begin{cases} 1 & \text{if } 0 \leq t < t_{sw} \\ 0 & \text{if } t_{sw} \leq t \end{cases}$
2	-	$z = 0 \forall t$ or $z = 1 \forall t$ or $z(t) = \begin{cases} 0 & \text{if } 0 \leq t < t_{sw} \\ 1 & \text{if } t_{sw} \leq t \end{cases}$
3	0	$z = 0 \forall t$ or $z = 1 \forall t$ or Singular Control

We consider a special case when $t_f \rightarrow \infty$. In this case, we can prove that a closed-form analytical solution exists. We propose the following:

Proposition 2. *For the first order system described in Eq.(51), with a closed-loop behavior of Eq.(52), a cost functional of Eq.(53), and*

an optimal switching sequence of Eq.(55), the following is true under the assumption that $a < 0$ and $(a - bk) < 0$, i.e., the open-loop and closed-loop systems are stable:

1. *If $(q_1bk + q_2a) > 0$, the optimal control is a bang-bang control that with at most one switching point. Furthermore, if $0 < -as/[(q_1bk + q_2a)x_0^2] < 1$, the optimal switching time is,*

$$t_{sw} = \frac{1}{2(a - bk)} \ln \left(\frac{-as}{(q_1bk + q_2a)x_0^2} \right) \quad (59)$$

If the inequality is not satisfied, the optimal control is $z^(t) = 0 \forall t$,*

2. *If $q_1bk + q_2a \leq 0$, the optimal control is $z^*(t) = 0 \forall t$.*

Proof for (1): Note from Eqs.(51) and (52) that the first order system will not produce $x = 0$ over a finite interval $t \in [t_1, t_2]$. Thus, a necessary condition for the existence of a singular interval, from Eq.(58), is $(q_1bk + q_2a) = 0$. Note that a singular interval corresponds to the ‘‘indeterminate’’ condition of Eq.(55) when valid over an interval $t \in [t_1, t_2]$. Since, in this case, $q_1bk + q_2a > 0$, therefore, a singular interval will not exist. Hence, from Eq.(55), the optimal control in this case is bang-bang control. From Eq.(58), $\alpha(t)$ is strictly increasing. Therefore, the optimal control has at most one switching point, as in Case 1 of Table 1. Assume that the switching time exists (denoted by t_{sw}), the optimal control can be expressed as,

$$z^*(t) = \begin{cases} 1 & \text{if } 0 \leq t < t_{sw} \\ 0 & \text{if } t_{sw} \leq t \end{cases} \quad (60)$$

We integrate Eq.(51) to find the expression of $x^*(t)$:

$$x^*(t) = \begin{cases} x_0 e^{(a-bk)t} & \text{if } 0 \leq t \leq t_{sw} \\ (x_0 e^{-bk t_{sw}}) e^{at} & \text{if } t > t_{sw} \end{cases} \quad (61)$$

The terminal condition of this problem is $\lambda(\infty) = (\partial\phi/\partial x) = 0$. Since we assume the system to be both open-loop and closed-loop stable, $x(\infty) \rightarrow 0$. Combining with the switching condition $\alpha(t_{sw}) = 0$, we have $\alpha(\infty) = s$. We can solve for the switching time t_{sw} :

$$\begin{aligned} \int_{t_{sw}}^{\infty} \dot{\alpha}(t) dt &= \alpha(\infty) - \alpha(t_{sw}) = s \\ \Rightarrow 2(q_1bk + q_2a)x_0^2 e^{-2bk t_{sw}} \int_{t_{sw}}^{\infty} e^{2at} dt &= s \\ \Rightarrow 2(q_1bk + q_2a)x_0^2 e^{-2bk t_{sw}} \left(-\frac{1}{2a} e^{2at_{sw}} \right) &= s \\ \Rightarrow e^{2(a-bk)t_{sw}} &= \frac{-as}{(q_1bk + q_2a)x_0^2} \\ \Rightarrow t_{sw} &= \frac{1}{2(a - bk)} \ln \left(\frac{-as}{(q_1bk + q_2a)x_0^2} \right) \end{aligned} \quad (62)$$

This equation shows that there is an analytical solution for the first-order infinite-time optimal problem. To guarantee the existence of the one-switching-point solution, the criterion for t_{sw} is $t_{sw} > 0$. From Eq.(62), the corresponding condition is $0 < -as/[(q_1bk + q_2a)x_0^2] < 1$. If the condition does not hold, the optimal control does not contain any switching point. Because the final time t_f tends to infinity, and $\alpha(\infty) = s > 0$, therefore the optimal control in this case is $z^*(t) = 0 \forall t$. \square

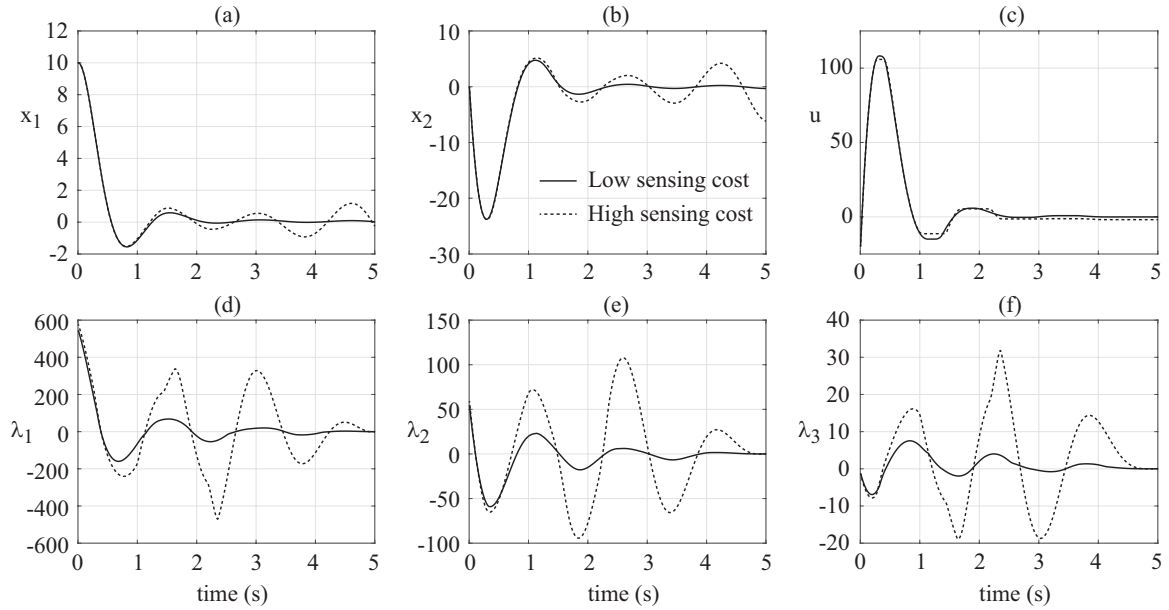


FIGURE 1 | States and Co-states for Simulations in Section 5.1 for Case 1: Low, and Case 2: High Sensing-Cost Weights

Proof for (2): First, consider the case $q_1bk + q_2a < 0$. From Table 1, the optimal control in this case can be one of the three solutions: $z(t) = 0 \forall t$, $z(t) = 1 \forall t$, or $z(t) = 0$ for $0 \leq t < t_{sw}$ and $z(t) = 1$ for $t_{sw} \leq t$. Note that since $t_f \rightarrow \infty$, only the solution $z(t) = 0 \forall t$ will yield bounded cost. Therefore, it is the optimal solution.

If $q_1bk + q_2a = 0$, we will prove the singular control does not exist in this case. If we have singular control on the sub-interval $t \in [t_1, t_2]$, then over that interval,

$$\frac{\partial H}{\partial z} = 0 \Rightarrow q_2x^2 + s - bk\lambda x = 0 \quad (63)$$

Note that the left-hand side of the equation above is the switching function $\alpha(t)$. From Eq.(58), we have $\dot{\alpha}(t) = 2(q_1bk + q_2a)x^2 = 0 \forall t$. Therefore, if the singular control exists, equation (63) holds for all $t > 0$. Recall from Proof of (1) that $\lim_{t \rightarrow \infty} x(t) = 0$. Also, $\lim_{t \rightarrow \infty} \lambda(t) = 0$ from the final condition on the co-states. Therefore,

$$\lim_{t \rightarrow \infty} \alpha(t) = \lim_{t \rightarrow \infty} (q_2x^2 + s - bk\lambda x) = s > 0 \quad (64)$$

This is a contradiction. Therefore, a singular control does not exist, $\alpha(t) = s \forall t$ and $z^*(t) = 0 \forall t$. \square

5 | Numerical Solution Examples

5.1 | Section 3.1 Example

In this example, we choose,

$$A = \begin{bmatrix} 0 & 1 \\ -16 & 1 \end{bmatrix}, B = \begin{bmatrix} 0 \\ 1 \end{bmatrix}, X(0) = \begin{bmatrix} 10 \\ 0 \end{bmatrix}, K = [2 \ 5] \quad (65)$$

Definitions of the matrices, and vectors in Eq.(65) can be found in Section 3.1. We consider two cases to compare results. In both cases, we use the same Q matrix. However, the sensing-cost

weight s is varied. The weights are:

$$Q = \begin{bmatrix} 100 & 0 \\ 0 & 0 \end{bmatrix}, s = \begin{cases} 1 & \text{Case 1: Low Sensing-Cost} \\ 1000 & \text{Case 2: High Sensing-Cost} \end{cases} \quad (66)$$

We recall that in this scenario, $u = -KX$ when $z = 1$, and $\dot{u} = 0$ when $z = 0$. For both cases of Eq.(66), the TPBVPs were solved using the ‘‘Relaxation Method’’ [13]. The simulation results are presented in Figs.1 and 2.

Figure 1 gives the state and co-state trajectories for the two cases. Figure 2 compares the control input u and the sensing/no-sensing switching state z for these cases. From Fig.2(b), it is clear that high sensing-cost leads to a smaller net sensing interval. The net sensing durations are,

$$\text{Case 1: } \int_0^5 z dt = 3.11s, \text{ Case 2: } \int_0^5 z dt = 1.175s \quad (67)$$

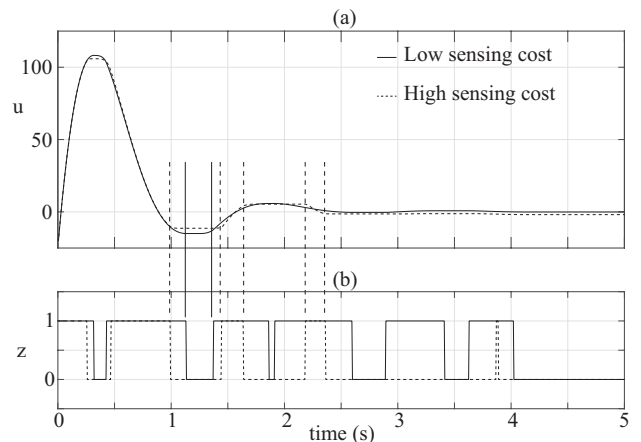


FIGURE 2 | Comparison of Control Input and Sensing State

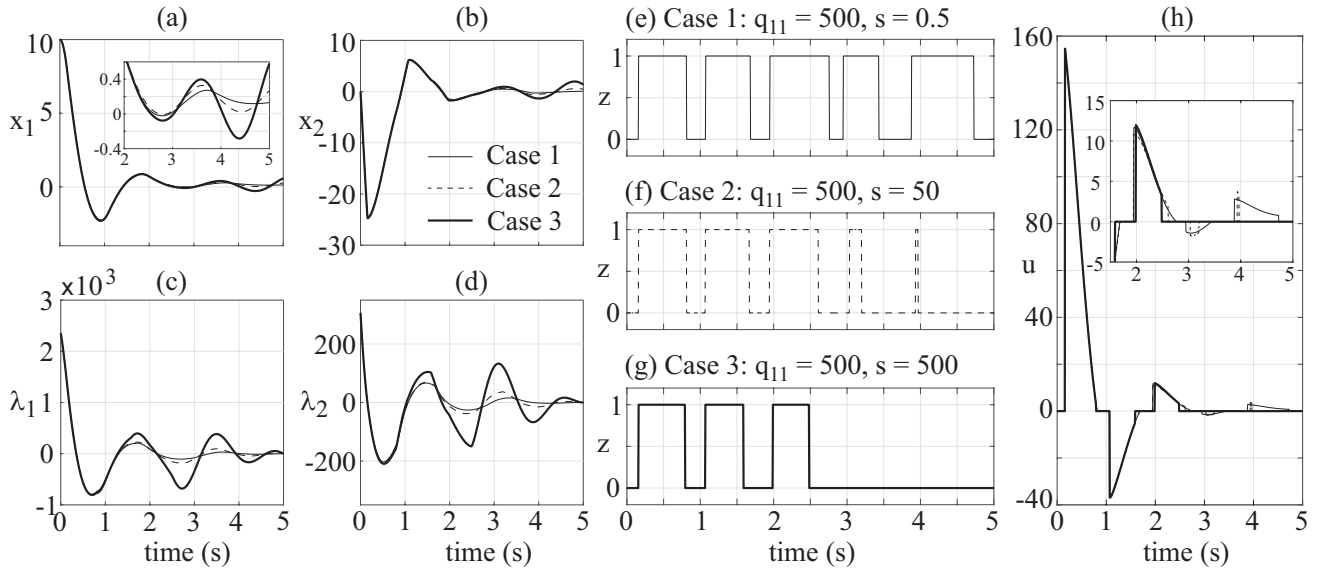


FIGURE 3 | Section 5.2 Simulation: States, Co-states, Switching Variable z and Control Input for Case 1: Low, Case 2: Intermediate, and Case 3: High Sensing-Cost

Figure 2(a) depicts some intervals when $z = 0$ for both cases, confirming that indeed $\dot{u} = 0$ when $z = 0$. In Eq.(65), while A is not Hurwitz, $(A - BK)$ is Hurwitz. Hence, we expect that when the sensing-cost is low, i.e. in Case 1, x_1 will be relatively more convergent to 0 than in Case 2, which applies a high sensing-cost. This is confirmed in Fig.1(a), where Case 2 causes x_1 to have a divergent trajectory. This divergence is because the stabilizing feedback $u = -KX$ is used for a shorter duration and almost not used after $t = 2.5$ s. Figure 1 also confirms the correct implementation of the boundary conditions for states and co-states, as given in Eq.(17).

5.2 | Section 3.2 Example

In this example, we choose,

$$A = \begin{bmatrix} 0 & 1 \\ -16 & 1 \end{bmatrix}, B = \begin{bmatrix} 0 \\ 1 \end{bmatrix}, X(0) = \begin{bmatrix} 10 \\ 0 \end{bmatrix}, K = [-7 \quad 4] \quad (68)$$

Recall from Section 3.2 that here we set $u = 0$ when $z = 0$ and $u = -KX$ when $z = 1$. We consider three cases to compare results. In all cases we use the same Q matrix. However, the sensing-cost weight s is varied. The weights are:

$$Q = \begin{bmatrix} 500 & 0 \\ 0 & 0 \end{bmatrix}, s = \begin{cases} 0.5 & \text{Case 1: Low Sensing-Cost} \\ 50 & \text{Case 2: Interm. Sensing-Cost} \\ 500 & \text{Case 3: High Sensing-Cost} \end{cases} \quad (69)$$

The TPBVPs for all cases of Eq.(69) were solved using the ‘‘Relaxation Method’’. The simulation results are presented in Fig.3. Figures 3(a)-(d) compare the state and co-state trajectories. Figures 3(e)-(g) plot the switching state z for the three cases. From Figs.3(e)-(g), it is clear that high sensing-cost s leads to a smaller

net sensing interval. The net sensing durations are,

$$\int_0^5 z dt = \begin{cases} \text{Case 1: } 3.41\text{s} \\ \text{Case 2: } 2.12\text{s} \\ \text{Case 3: } 1.65\text{s} \end{cases} \quad (70)$$

The effect of lesser sensing can be seen in the state variables, especially in x_1 in Fig.3(a). The inset in Fig.3(a) shows that x_1 performance is progressively degraded as s increases. This is due to lesser use of the stabilizing control, $u = -KX$. Note that in this example, A is not Hurwitz but $(A - BK)$ is. Figure 3 also confirms the correct implementation of the boundary conditions for states and co-states, as given in Eq.(27). Figure 3(h) compares the control inputs for the three cases. The inset figure in Fig.3(h) shows progressively shorter duration of control application from Case 1 to 3.

5.3 | Section 3.3 Example

In this example, we choose,

$$A = \begin{bmatrix} 0 & 1 \\ -16 & 1 \end{bmatrix}, B = \begin{bmatrix} 0 \\ 1 \end{bmatrix}, X(0) = \begin{bmatrix} 10 \\ 0 \end{bmatrix} \quad (71)$$

Recall from Section 3.3 that here we set $u = 0$ when $z = 0$ and $u = u^*$, Eq.(35), when $z = 1$. We consider three cases to compare results. In all cases we use the same Q matrix. However, the weights R and s are varied. The weights are:

$$Q = \begin{bmatrix} 5000 & 0 \\ 0 & 0 \end{bmatrix}, s = \begin{cases} \text{Case 1: } 0.5 \\ \text{Case 2: } 50 \\ \text{Case 3: } 50 \end{cases}, R = \begin{cases} \text{Case 1: } 5 \\ \text{Case 2: } 5 \\ \text{Case 3: } 50 \end{cases} \quad (72)$$

The TPBVPs for all cases of Eq.(72) were solved using the ‘‘Relaxation Method’’. The simulation results are presented in Fig.4. Figures 4(a)-(d) compare the state and co-state trajectories. Figures 4(e)-(g) plot the switching state z for the three cases. The

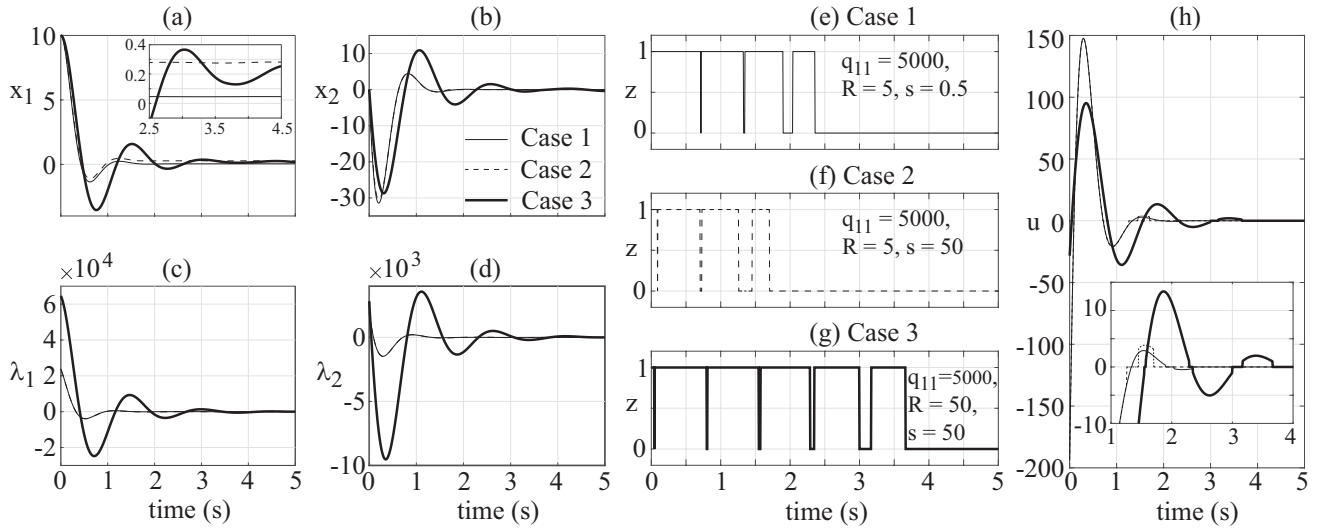


FIGURE 4 | Section 5.3 Simulation: States, Co-states, Switching Variable z and Control Input for Cases: 1, 2 and 3

net sensing durations are,

$$\int_0^5 z dt = \begin{cases} \text{Case 1: } 2.195\text{s} \\ \text{Case 2: } 1.48\text{s} \\ \text{Case 3: } 3.395\text{s} \end{cases} \quad (73)$$

The integral control effort for the three cases are:

$$\int_0^5 z u^2 dt = \int_0^5 z (-0.5R^{-1}B^T\lambda)^2 dt = \begin{cases} \text{Case 1: } 1.45 \times 10^6 \\ \text{Case 2: } 1.44 \times 10^6 \\ \text{Case 3: } 7.77 \times 10^5 \end{cases} \quad (74)$$

Note that from Case 1 to 2, the cost of sensing was increased from $s = 0.5$ to $s = 50$. This caused the sensing duration to decrease, as evident from Eq.(73). Between Cases 1 and 2, note that the integral control effort remains approximately unchanged, as evident from Eq.(74). From Case 2 to 3, the cost of control was increased from $R = 5$ to $R = 50$. As expected, this led to a reduction in the integral control effort, as seen in Eq.(74). The state x_1 in Fig.4(a) shows an interesting behavior between the three cases. From Case 1 and 2, we observe that steady-state behavior of x_1 degrades. This is attributed to the higher sensing-cost s in Case 2. However, from Case 2 to 3, we notice a degradation in the transients. This is due to the increase in R which leads to lower control effort in Case 3. This is also reflected in the control inputs plotted in Fig.4(h). Compared to Cases 1 and 2, the control input signal of Case 3 has lower magnitudes due to a higher R value. The inset figure in Fig.4(h) confirms that the control input switches to zero when $z = 0$.

5.4 | Section 4.1 Example

This section presents simulation results for a first-order system with the following parameters:

$$\begin{aligned} a &= -1, & b &= 1, & k &= 1, & x_0 &= 10, \\ q_1 &= 1, & q_2 &= 0, & s &= 1, & t_f &= 10. \end{aligned} \quad (75)$$

The example uses a built-in function in MATLAB named *bvp4c* to solve the TPBVP numerically. It is implemented using the

three-stage Lobatto IIIa formula and the fourth-order forward integration ([17]). From the analytical result of Eq.(62), the optimal switching time is $t_{sw}^* = 1.15129$ sec, which is very close to the result shown in Fig.5(a). The difference between the results is due to: (1) The function *bvp4c* uses an approximate method for time-integration, and (2) The end time of the numerical simulation ($t_f = 10$ s) is finite.

Another validation result is illustrated in Fig.5(b), where the system dynamics is directly simulated at varying switching instants. The switching time is swept with each step of 1ms. The total cost is calculated at each step following Eq.(53). The result shows that the optimal switching time is $t_{sw,opt} = 1.151$ sec, which matches the results mentioned above. Figure 5(a) also shows the optimal solution for $s = 100$ obtained numerically. For the parameters chosen and the criterion for the existence of a t_{sw} , i.e., $s < -((q_1bk + q_2a)x_0^2/a)$, we note that t_{sw} exists if $s < 100$. Accordingly, in the case of $s = 100$, the optimal solution should be $z = 0 \forall t$. This is in agreement with the solution in Fig.5(a).

6 | A Practical Example: Waste Water Treatment Plant

Human activities are increasing the concentrations of nitrogen and phosphorus in the environment. Excessive levels of these nutrients lead to water pollution, causing adverse effects on human health, environmental degradation, and economic losses [18]. Waste water treatment plants (WWTPs) play a critical role in removing nitrogen and phosphorus from water. In these systems, water quality sensors, such as those measuring ammonia and nitrate concentrations, are costly and require regular maintenance. This motivates the application of a sensing cost framework to minimize the total sensor usage time while preserving the performance of the WWTP.

In this section, we consider a linearized WWTP model around the nominal operating point defined by the ammonia and nitrate concentrations. We incorporate sensing cost into an output feedback control scheme to reduce sensor usage time while maintaining control performance near the nominal operating condition.

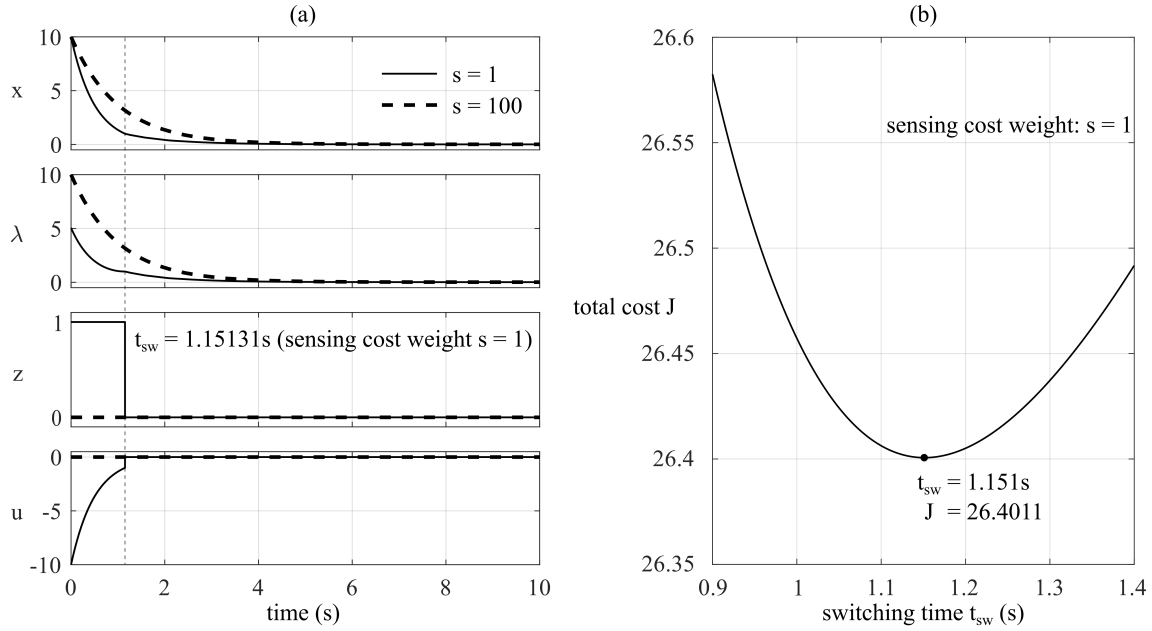


FIGURE 5 | Numerical solution for Sec. 4.1 example

6.1 | State-space representation

From [18], the MIMO transfer function matrix of a WWTP can be expressed as:

$$\begin{bmatrix} Y_1(s) \\ Y_2(s) \end{bmatrix} = \begin{bmatrix} p_{w11}(s) & p_{w12}(s) \\ p_{w21}(s) & p_{w22}(s) \end{bmatrix} \begin{bmatrix} U_1(s) \\ U_2(s) \end{bmatrix} \quad (76)$$

Where the outputs $y_1(t)$ and $y_2(t)$ are the concentration of ammonia (NH_4) and nitrates (NO_3) in the effluent, respectively, the input $u_1(t)$ is the air flow injected in the aerobic tank and $u_2(t)$ is the external sludge recirculation flow from settler to anaerobic tank. The transfer function $p_{wij}(s)$, $i, j \in \{1, 2\}$ are obtained by linearizing the WWTP model about the working point, where the concentrations of ammonia and nitrates are 1 and 4 g/m^3 , respectively.

$$\begin{aligned} p_{w11}(s) &= \frac{k_{11}}{1 + s/a_{11}} \\ p_{w12}(s) &= \frac{k_{12}(1 + s/z_{12,1})(1 + s/z_{12,2})}{(1 + s/a_{12})[1 + (2\zeta_{12}^2/\omega_{n12})s + (s/\omega_{n12})^2]} \\ p_{w21}(s) &= \frac{k_{21}}{1 + s/a_{21}}, \quad p_{w22}(s) = \frac{k_{22}}{1 + s/a_{22}} \end{aligned} \quad (77)$$

where the parameters are:

- $k_{11} = -0.04$, $a_{11} = 7.25 \times 10^{-5}$.
- $k_{12} = -6.239 \times 10^{-4}$, $z_{12,1} = 7.534 \times 10^{-4}$, $z_{12,2} = -3.17 \times 10^{-5}$, $\omega_{n12} = 4.58 \times 10^{-4}$, $\zeta_{12} = 0.8493$.
- $k_{21} = 0.0464$, $a_{21} = 1.008 \times 10^{-4}$.
- $k_{22} = -2 \times 10^{-5}$, $a_{22} = 1.67 \times 10^{-4}$.

Because there are three first-order and one third-order transfer functions, a state-space representation with order 6 can be

employed to describe this system:

$$\begin{cases} \dot{X} = AX + BU \\ Y = CX + DU \end{cases} \quad (78)$$

where:

$$\begin{aligned} A &= \begin{bmatrix} -7.25 \times 10^{-5} & \mathbf{0}_{1 \times 3} & 0 & 0 \\ \mathbf{0}_{3 \times 1} & A_{12} & \mathbf{0}_{3 \times 1} & \mathbf{0}_{3 \times 1} \\ 0 & \mathbf{0}_{1 \times 3} & -1.008 \times 10^{-4} & 0 \\ 0 & \mathbf{0}_{1 \times 3} & 0 & -1.67 \times 10^{-4} \end{bmatrix} \\ A_{12} &= \begin{bmatrix} 0 & 1 & 0 \\ 0 & 0 & 1 \\ -1.687 \times 10^{-11} & -2.723 \times 10^{-7} & -8.584 \times 10^{-4} \end{bmatrix} \\ B &= \begin{bmatrix} -2.9 \times 10^{-6} & 0 \\ 0 & 0 \\ 0 & 0 \\ 4.677 \times 10^{-6} & 0 \\ 0 & -3.34 \times 10^{-9} \end{bmatrix} \\ C &= \begin{bmatrix} 1 & -1.052 \times 10^{-16} & 3.18 \times 10^{-12} & 4.406 \times 10^{-9} & 0 & 0 \\ 0 & 0 & 0 & 0 & 1 & 1 \end{bmatrix} \\ D &= \mathbf{0}_{2 \times 2} \end{aligned}$$

We assume that only the outputs can be measured, therefore, we propose an output-feedback control:

$$U = -K_y Y = \begin{bmatrix} K_{y11} & K_{y12} \\ K_{y21} & K_{y22} \end{bmatrix} \begin{bmatrix} y_1 \\ y_2 \end{bmatrix} \quad (80)$$

To determine the gain matrix K_y , we first apply relative gain array (RGA) analysis to assess the input-output pairings. The result indicates that, in the low-frequency range, the diagonal pairing (use u_1 to control y_1 and u_2 to control y_2) is appropriate for controlling the MIMO system. Based on trial-and-error tuning, the gain matrix is selected as $K_y = -10I_2$. Denote $z \in \{0, 1\}$ as the

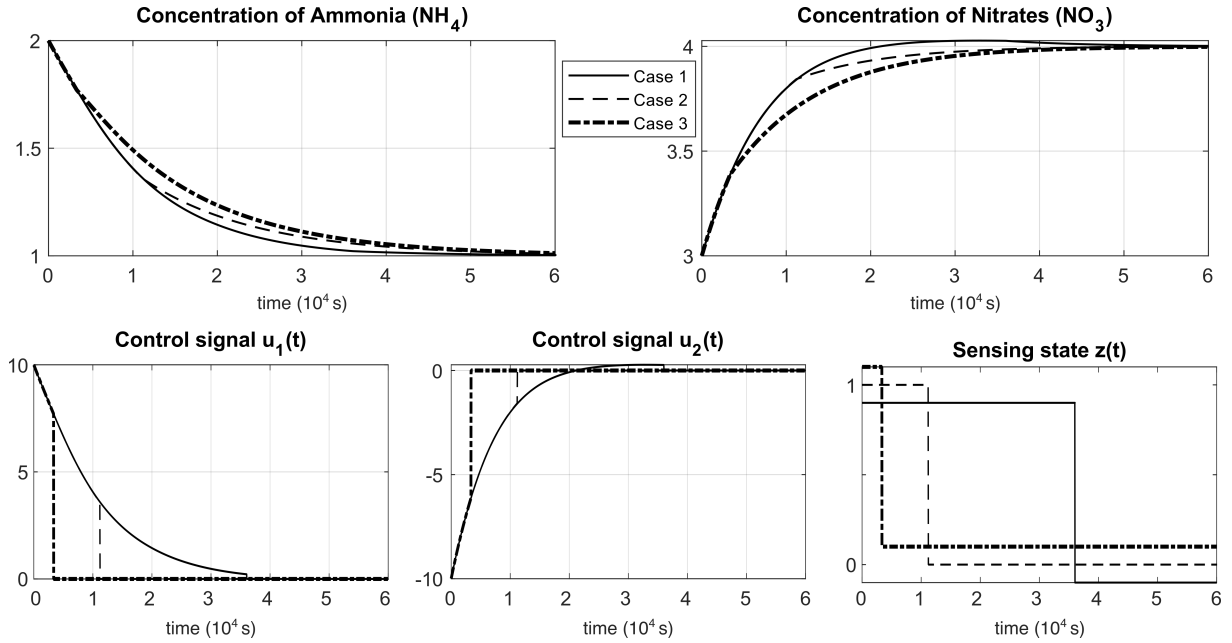


FIGURE 6 | Simulation results for three sensing cost values: low ($s = 0.001$), intermediate ($s = 0.1$), and high ($s = 0.5$). Concentration plots show true concentrations (not outputs y_1 and y_2), and the sensing state $z(t)$ plots are offset for clarity

sensing state, we will find the optimal sequence $z^*(t)$ to optimize the following cost functional:

$$J = \int_{t_0}^{t_f} (Y^T Q_y Y + sz) dt = \int_{t_0}^{t_f} (X^T \underbrace{C^T Q_y C}_Q X + sz) dt \quad (81)$$

By applying the results presented in section 3.2, we have the co-state differential equation:

$$\begin{aligned} \dot{\lambda} &= -2C^T Q_y C X - (A - zBK_y C)^T \lambda \\ &= -2C^T Q_y Y - (A - zBK_y C)^T \lambda \end{aligned} \quad (82)$$

and the switching condition:

$$z = \begin{cases} 1 & \text{when } s < \lambda^{*T} B K_y Y^* \\ 0 & \text{when } s > \lambda^{*T} B K_y Y^* \end{cases} \quad (83)$$

6.2 | Simulation Results

We use the MATLAB built-in function *bvp4c* to simulate the WWTP model in a time span of 60000 seconds. The initial condition of the state vector is set at $X_0 = [9.634 \times 10^{-1}, -3.483 \times 10^{14}, 1.665 \times 10^2, 2.96 \times 10^{-1}, -1.117, 1.175 \times 10^{-1}]$, which corresponds to a starting point with the output of $Y(0) = [1, -1]^T$. The chosen output cost matrix is $Q_y = I_2$. The simulation is conducted for three different values of the sensing cost coefficient s :

$$s = \begin{cases} 0.001 & \text{Case 1: Low sensing cost} \\ 0.1 & \text{Case 2: Intermediate sensing cost} \\ 0.5 & \text{Case 3: High sensing cost} \end{cases}$$

Figure 6 and Table 2 illustrate the comparison among three scenarios. When the sensing cost is incorporated into the model, a trade-off between output cost and sensing cost can be observed.

As the sensing cost increases (i.e., sensing becomes more expensive), the optimal total sensing duration decreases to minimize the overall cost. In addition, as the sensing cost coefficient increases, the output performance degrades, as shown in Fig. 6. Specifically, a higher sensing cost leads to a longer settling time, as well as a higher output cost, as indicated in Table 2.

TABLE 2 | Performance comparison between three cases

Case	Output cost	Net sensing duration (s)
1	8984	36033
2	9288	11209
3	11035	3364

7 | A Shrinking Horizon Implementation

All of the solutions presented in Section 3 and examples in Section 5 are considered *offline* solutions, meaning that the optimal sequence of z is pre-calculated based on a known, precise system model and initial conditions. Then, using the pre-calculated switching times, sensing can be switched on or off and inputs accordingly applied. In practice however, a system is always subject

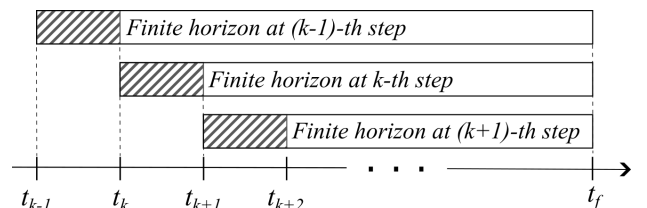


FIGURE 7 | Shrinking horizon scheme (adapted from [19])

to uncertainties, which leads to sub-optimal performance when the offline solution is implemented. This issue is compounded for the problem addressed in Section 3.3, where the optimal input of Eq.(35) is not directly a state feedback control. As a result, even when $z = 1$, it is not explicit from Eq.(35) how sensing is helpful. A *Shrinking Horizon* (SH) implementation is a practical way to address this issue ([19] and [20]).

In the *Shrinking Horizon* method, the time span $[t_0, t_f]$ is evenly divided into multiple steps. Initially, we assume that the state $X(t_0) = X_0$ is known and we solve the optimal problem by using the numerical methods presented in Section 5. If the resulting optimal sensing state at the initial time is $z = 1$, we apply the feedback control and the next initial state $X(t_1)$ is known (i.e., sensed). Conversely, if $z = 0$, we apply the appropriate control input (i.e. $u = [0]$ or $\dot{u} = [0]$), but do not sense $X(t_1)$. However, since the system model is given (albeit, may not be accurate), we can integrate the system model to get the calculated state $X_{cal}(t_1)$. We choose this state as the new initial condition and solve the optimal control problem (i.e., the TPBVP) for a time span $[t_1, t_f]$, which is over a shrinking time horizon. We repeat this process until we reach the final time step $k = N$ (Fig. 7).

We first demonstrate the Shrinking Horizon (SH) implementation for the first-order system introduced in Section 5.4 and Eq.(75). This allows direct comparison with the analytical solution. The SH is implemented in a time spans of 10 sec, discretized into 1000 steps with a sampling time of 0.01 sec. When the model parameters are perfectly known, it is straightforward that the SH implementation produces results identical to the single-step TPBVP solution.

Next, we introduce uncertainties in the system. We assume that the *true model* can be formulated as,

$$\dot{x}_{true}(t) = (a + \delta a)x_{true} + (b + \delta b)u \quad (84)$$

In this simulation, the uncertainty parameters are constant bias set to $\delta a = 0.2$, $\delta b = 0.1$. Applying Eq.(62), the optimal switching time is calculated to be $t_{sw} = 1.29$ seconds. As shown in Fig.8, the switching time for SH implementation and TPVBP methods are at 1.22s and 1.15s, respectively. Since the switching time derived from the SH method is consistent with the global optimum

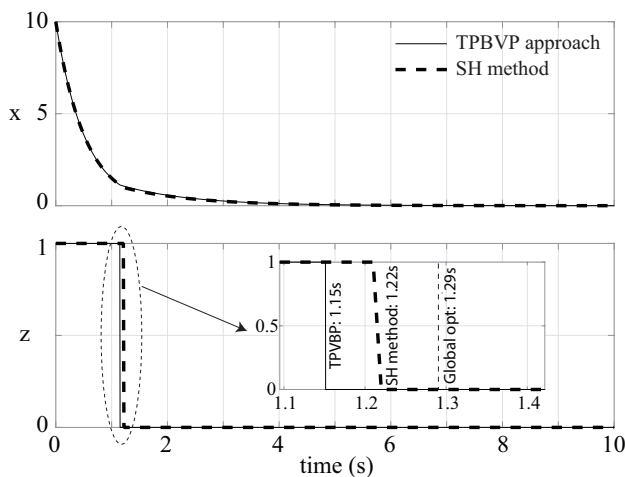


FIGURE 8 | Comparison between TPBVP and Shrinking Horizon implementation, first-order system (with model uncertainties $\delta a = 0.2$, $\delta b = 0.1$)

as well as the TPBVP solution, this indicates that the method is suitable for handling practical problems involving switching cost impositions, including ones that involve uncertainties.

Next, consider the unstable second-order system introduced in Section 5.2, given by Eqs.(68)–(69) (Case 2: $s = 50$). To demonstrate the adaptivity of the Shrinking Horizon method, the uncertainties of about 3% to 5% are introduced into the system matrices A and B as follows:

$$A_{true} = A + \delta A = \begin{bmatrix} 0 & 1 \\ -16 & 1 \end{bmatrix} + \begin{bmatrix} 0 & 0 \\ 0.7 & -0.03 \end{bmatrix} = \begin{bmatrix} 0 & 1 \\ -15.3 & 0.97 \end{bmatrix} \quad (85)$$

$$B_{true} = B + \delta B = \begin{bmatrix} 0 \\ 1 \end{bmatrix} + \begin{bmatrix} 0 \\ -0.05 \end{bmatrix} = \begin{bmatrix} 0 \\ 0.95 \end{bmatrix} \quad (86)$$

In this example, the 5-second time span is divided into 500 steps, each with a sampling time of 0.01 sec. Figure 9 compares the performance of the single TPBVP approach, the SH implementation, and the TPBVP solution of the true model (used as a reference). The total cost J for each method is as follows: the single TPBVP approach yields $J = 12656$, the SH implementation results in $J = 12354$, and the TPBVP for true model achieves the lowest cost with $J = 12301$. The SH method reduces the cost by 302 units relative to the single TPBVP, recovering over 85% of the performance loss caused by model uncertainty. The state trajectories $x_1(t)$ and $x_2(t)$ show that the SH method effectively compensates for errors introduced by model uncertainty. While the single TPBVP exhibits unstable behavior unsuitable for long-term operation, the SH implementation maintains stability of the state vector $[x_1, x_2]^T$. This performance gain demonstrates the SH methods ability to better track the optimal trajectory in uncertain environments. However, the SH result may exhibit chattering (high-frequency oscillations), as observed at $t = 2$ s. This occurs when the sensing state z switches from 0 to 1 (or vice versa), potentially causing a mismatch between the guessed state (propagated using the nominal matrices A and B) and the sensed state (according to the true model $\dot{X}_{true} = A_{true}X_{true} + B_{true}u$). This behavior should be further investigated to ensure the robustness of the control scheme. As in the first-order case, this simple example illustrates the feasibility of the SH approach and hints at its potential for more complex systems with switching costs.

While the cases presented here are basic, further investigation across a wider range of systems is needed to fully assess its viability. Nevertheless, these results confirm the basic feasibility of the method and its suitability for the formulation in Sec. 3.3, where, whenever $z = 1$, the SH implementation uses the measured $X(t)$ to solve the TPBVP and obtain $\lambda(t)$ for use in Eq. (35).

8 | Conclusion

This study presents a novel optimal control framework for LTI systems that incorporates cost of sensing in its performance index. In this introductory work, a binary switching variable, z , toggles state-sensing between active ($z = 1$) and inactive ($z = 0$). For each scenario, distinct control input formulations are examined. During active sensing, we consider a predefined state-feedback control and an optimal control. During inactive sensing, we explore zero input ($u = [0]$) and constant input $\dot{u} = [0]$. The switching sequence of z is optimized to minimize a cost functional incorporating penalties on system states, control effort,

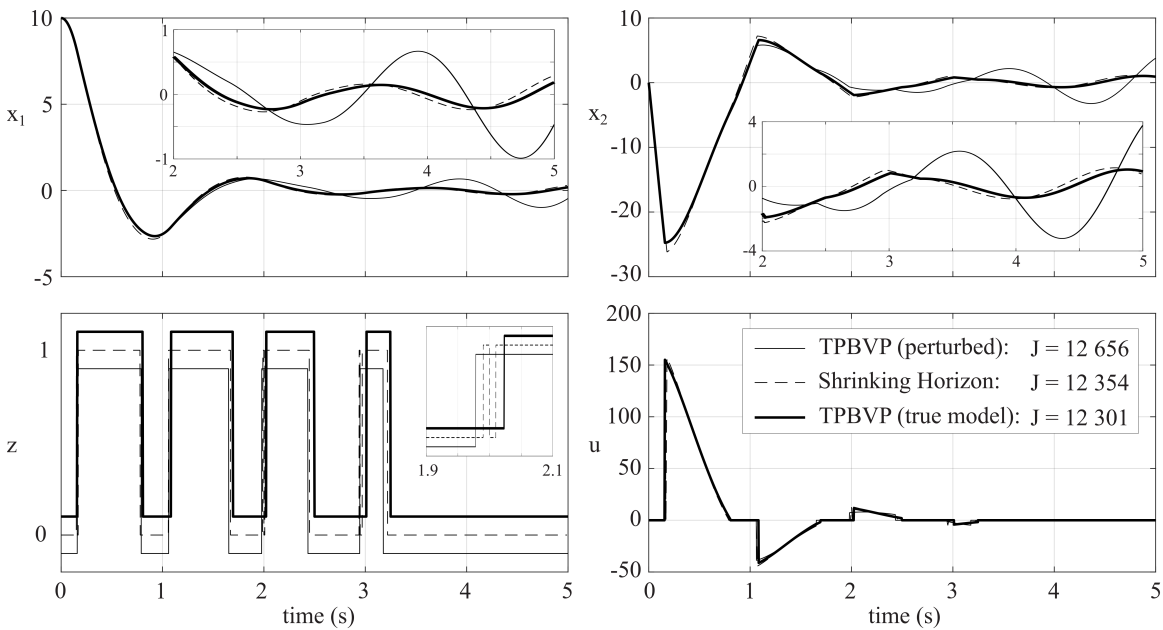


FIGURE 9 | Comparison between TBPVP and Shrinking Horizon, second-order system with model uncertainty. Note that the z-plots have different offsets for easier distinction

and sensing duration. This optimization is achieved using the Pontryagin's Minimum Principle.

Various numerical simulations were conducted to validate the proposed framework. In Section 5.1, where a stabilizing feedback, $u = -KX$ is employed during active sensing and input is held constant during inactive sensing, very high penalties on sensing-cost resulted in divergent trajectories due to insufficient sensing duration. This observation underscores the importance of carefully selecting the weight of sensing-cost. Section 5.3 demonstrates that a joint optimization can effectively balance sensing-costs, control efforts, and state stabilization, ensuring a balanced trade-off between system performance and resource utilization. A reduced-form equation for the infinite-horizon multi-dimensional case with single switching point is derived, and a closed-form solution is obtained for the infinite-horizon first-order case. An example for the first-order system is also provided to validate the derived closed-form solution, and a practical waste water treatment plant example is presented to demonstrate the applicability of the framework to systems with costly, maintenance-intensive sensors.

The resulting TPBVPs are initially solved offline, with optimal sensing schedules pre-computed assuming accurate system models. However, this offline approach may be impractical and yield suboptimal results in the presence of uncertainties. To address this, a Shrinking Horizon approach is taken, solving the optimal control problem at each time step while updating the initial state based on the sensing status. Simulations show that this method achieves switching times comparable to the offline TPBVP solutions, highlighting its potential for practical applications. Finally, we note that the proposed framework is formulated over a fixed finite time horizon and focuses on cost-based optimality rather than asymptotic stabilization. As a result, open-loop unstable systems can be considered over the horizon of interest. While the current work focuses on LTI systems, the theoretical framework provides a strong foundation for extending the proposed approach to more complex systems. Additional formulations of

sensing cost, such as selective sensing, switching between state and output feedback (e.g., via observers), and open-loop estimation, are possible extensions.

Funding

The authors declare that no external funding was received for this work.

Conflicts of Interest

The authors declare that they have no known competing financial interests or personal relationships that could have appeared to influence the work reported in this paper.

Data availability statement

The data that support the findings of this study are available from the corresponding author upon reasonable request.

References

1. E. Clark, T. Askham, S. L. Brunton, and J. N. Kutz. "Greedy Sensor Placement With Cost Constraints." *IEEE Sensor Journal*, vol. 19, no. 7 (2019): 2642–2656. doi: <https://doi.org/10.1109/JSEN.2018.2887044>.
2. T. Das and R. Mukherjee. "Shared-Sensing and Control Using Reversible Transducers." *IEEE Transactions on Control Systems Technology*, vol. 17, no. 1 (2009): 242–248. doi: <https://doi.org/10.1109/TCST.2008.924570>.
3. V. Ganesan, T. Das, N. Rahnavard, and J. L. Kauffman. "Vibration-based monitoring and diagnostics using compressive sensing." *Journal of Sound and Vibration* 394 (2017): 612–630. doi: <https://doi.org/10.1016/j.jsv.2017.02.002>.
4. V. Gupta, T. H. Chung, B. Hassibi, and R. M. Murray. "On a stochastic sensor selection algorithm with applications in sensor scheduling and sensor coverage." *Automatica*, vol. 42, no. 2 (2006): 251–260. doi: <https://doi.org/10.1016/j.automatica.2005.09.016>.

5. A. V. Savkin, R. J. Evans, and E. Skafidas. 2001. “The problem of optimal robust sensor scheduling.” In *Proceedings of the 39th IEEE Conference on Decision and Control (Cat. No.00CH37187)*, Vol 4, 3791–3796. doi: <https://doi.org/10.1109/CDC.2000.912300>.
6. W. P. M. H. Heemels, K. H. Johansson, and P. Tabuada. 2012. “An introduction to event-triggered and self-triggered control.” In *IEEE 51st Conference on Decision and Control (CDC)*, 3270–3285. doi: <https://doi.org/10.1109/CDC.2012.6425820>.
7. R. K. Boel and J. H. van Schuppen. 2015. “Optimal control and optimal sensor activation for Markov decision problems with costly observations.” In *2015 IEEE Conference on Control Applications (CCA)*, 1440–1447. doi: <https://doi.org/10.1109/CCA.2015.7320814>.
8. D. E. Kirk 1970. *Optimal control theory: an introduction*, Prentice-Hall.
9. A. E. Bryson and Y. C. Ho. 1975. *Applied Optimal Control*, Hemisphere Publishing Corporation, Washington, D. C.
10. R. F. Stengel 1994. *Optimal Control and Estimation*, Dover Publications, Mineola, NY.
11. F. L. Lewis, D. L. Vrabie, and V. L. Syrmos. 2012. *Optimal Control*, John Wiley & Sons, Ltd. doi: <https://doi.org/10.1002/9781118122631>.
12. T. Das and R. Mukherjee. “Optimally switched linear systems.” *Automatica*, vol. 44, no. 5 (2008): 1437–1441. doi: <https://doi.org/10.1016/j.automatica.2007.10.008>.
13. W. H. Press, S. A. Teukolsky, W. T. Vetterling, and B. P. Flannery. 1992. *Numerical Recipes in C: The Art of Scientific Computing*, Cambridge University Press, New York, NY.
14. T. Das, R. Mukherjee, and J. Cameron. “Optimal Trajectory Planning for Hot-Air Balloons in Linear Wind Fields.” *Journal of Guidance, Control, and Dynamics*, vol. 26, no. 3 (2003): 416–424. doi: <https://doi.org/10.2514/2.5079>.
15. R. A. Horn and C. R. Johnson. 2013. *Matrix Analysis*, Cambridge University Press, 32 Avenue of the Americas, New York, NY 10013-2473.
16. P. J. Antsakalis and A. N. Michel. 1997. *Linear Systems*, McGraw-Hill, Englewood Cliffs, NJ.
17. J. Kierzenka and L. F. Shampine. “A BVP solver based on residual control and the Matlab PSE.” *ACM Transactions on Mathematical Software (TOMS)*, vol. 27, no. 3 (2001): 299–316. doi: <https://doi.org/10.1145/502800.502801>.
18. M. García-Sanz 2017. *Robust Control Engineering: Practical QFT Solutions*, CRC Press. doi: <https://doi.org/10.4324/9781315394985>.
19. A. Capannolo, G. Zanotti, M. Lavagna, and G. Cataldo. “Model predictive control for formation reconfiguration exploiting quasi-periodic tori in the cislunar environment.” *Journal of Non-linear Dynamics*, vol. 111, no. 8 (2023): 6941–6959. doi: <https://doi.org/10.1007/s11071-022-08214-8>.
20. J. Skaf, S. Boyd, and A. Zeevi. “Shrinking-horizon dynamic programming.” *International Journal of Robust and Nonlinear Control*, vol. 20, no. 17 (2010): 1993–2002. doi: <https://doi.org/10.1002/rnc.1566>.